

p53 Counteracts reprogramming by inhibiting mesenchymal-to-epithelial transition

R Brosh^{*1,2,3}, Y Assia-Alroy^{1,3}, A Molchadsky¹, C Bornstein¹, E Dekel¹, S Madar¹, Y Shetzer¹, N Rivlin¹, N Goldfinger¹, R Sarig¹ and V Rotter¹

The process of somatic cell reprogramming is gaining increasing interest as reprogrammed cells are considered to hold a great therapeutic potential. However, with current technologies this process is relatively inefficient. Recent studies reported that inhibition of the p53 tumor suppressor profoundly facilitates reprogramming and attributed this effect to the ability of p53 to restrict proliferation and induce apoptosis. Given that mesenchymal-to-epithelial transition (MET) was recently shown to be necessary for reprogramming of fibroblasts, we investigated whether p53 counteracts reprogramming by affecting MET. We found that p53 restricts MET during the early phases of reprogramming and that this effect is primarily mediated by the ability of p53 to inhibit Klf4-dependent activation of epithelial genes. Moreover, transcriptome analysis revealed a large transcriptional signature enriched with epithelial genes, which is markedly induced by Klf4 exclusively in p53^{-/-} cells. We also found that the expression of the epithelial marker E-Cadherin negatively correlates with p53 activity in a variety of mesenchymal cells even before the expression of reprogramming factors. Finally, we demonstrate that the inhibitory effect of p53 on MET is mediated by p21. We conclude that inhibition of the p53–p21 axis predisposes mesenchymal cells to the acquisition of epithelial characteristics and renders them more prone to reprogramming. Our study uncovers a novel mechanism by which p53 restrains reprogramming and highlights the role of p53 in regulating cell plasticity.

Cell Death and Differentiation (2013) 20, 312–320; doi:10.1038/cdd.2012.125; published online 21 September 2012

The tumor suppressor p53 is a pivotal transcription factor that promotes cell-cycle arrest, DNA-repair, senescence and apoptosis in response to a variety of stress signals.¹ The majority of p53 functions are mediated by transcriptional activation of target genes, among which, p21 is crucial for the suppression of cell division and for transcriptional repression.^{1,2} Recent evidence indicates that the function of p53 is not restricted to the aforementioned classical tumor-suppressive activities; and extends to the regulation of differentiation and development.³ While early studies reported that cancer-prone p53^{-/-} mice develop normally,⁴ subsequent detailed analyses indicated that in many cases, they exhibit developmental defects, such as exencephaly, polydactyly of the hind limbs, craniofacial malformations, ocular abnormalities, defects in the upper incisor teeth,^{5,6} as well as reduced fertility.⁷ Importantly, p53 can activate or suppress differentiation in a cell type- and fate-dependent manner, not only by mediating cell-cycle arrest and apoptosis, but also via direct transcriptional regulation of differentiation factors. Accordingly, several studies unveiled roles for p53 in well-characterized *in-vitro* differentiation models, including myogenic, osteogenic, neuronal, hematopoietic and adipogenic differentiation, as well as in the regulation of embryonic stem cell (ESC) differentiation.³

Apart from governing differentiation pathways, p53 was shown to participate in processes involving de-differentiation, and specifically, in reprogramming. Reprogramming of somatic cells into induced pluripotent stem cells (iPSCs) by ectopic expression of defined transcription factors, such as Pou5f1 (Oct4), Sox2, Klf4 and Myc, was pioneered by Takahashi and Yamanaka.⁸ Reprogramming represents a clear example of a process in which cells undergo complete de-differentiation, starting from a terminally differentiated state and culminating as pluripotent cells. Although iPSCs hold promise as a therapeutic tool, a major drawback of reprogramming lies in its inefficiency. Thus, in search of methods to improve this technique and in order to understand its underlying mechanisms, several groups have recently investigated the role of p53 in this complex process, revealing that the inhibition of p53, as well as its primary target gene p21, markedly facilitates and expedites reprogramming of mouse and human cells.^{9–14} These studies proposed possible mechanisms by which the p53–p21 axis restricts iPSCs generation, including induction of cell-cycle arrest, apoptosis and senescence. Hanna *et al.*¹⁴ described reprogramming as a stochastic process defined by two elements; an intrinsic cell type-specific constant and proliferation rate. In this context,

¹Department of Molecular Cell Biology, Weizmann Institute of Science, Rehovot, Israel and ²Department of Developmental and Regenerative Biology, The Black Family Stem Cell Institute, Mount Sinai School of Medicine, New York, NY, USA

*Corresponding author: R Brosh, Department of Molecular Cell Biology, Weizmann Institute of Science, PO Box 26, Rehovot 76100, Israel. Tel: 972 8 934 4501; Fax: 972 8 946 5265; E-mail: ranbroshran@gmail.com

³These authors contributed equally to this work.

Keywords: p53; p21; Klf4; reprogramming; MET

Abbreviation: ESC, embryonic stem cells; MEF, mouse embryonic fibroblasts; QRT-PCR, quantitative real-time PCR; MET, mesenchymal-to-epithelial transition; EMT, epithelial-to-mesenchymal transition; TGF β , transforming growth factor β ; iPSC, induced pluripotent stem cells; Klf4, Krüppel-like factor 4; shRNA, small hairpin RNA

Received 17.2.12; revised 30.7.12; accepted 27.8.12; Edited by G Melino; published online 21.9.12

p53 deficiency was suggested to merely affect proliferation rate and not the intrinsic constant. Notably, despite the potential of p53 inhibition to enhance reprogramming efficiency, reprogramming of p53-compromised cells can yield defective iPSCs with chromosomal aberrations and genome instability.¹⁰ Moreover, studies showed that the increase in reprogramming efficiency using p53-deficient and mutant-p53 expressing cells is associated with malignant transformation,^{13,15} highlighting the link between reprogramming and tumorigenesis. It appears that in both processes p53 functions to eliminate potentially hazardous cells by regulating proliferation and death. It still remains unclear whether p53 also affects the process of de-differentiation that underlies reprogramming and may accompany transformation.

Mesenchymal-to-epithelial transition (MET) was recently shown to initiate and to be required for reprogramming of fibroblasts.^{16,17} Accordingly, keratinocytes and mammary gland cells, both of epithelial origin, give rise to iPSCs more efficiently than fibroblasts.^{17,18} Mesenchymal and epithelial cells differ in multiple characteristics. Mesenchymal cells are usually elongated, spindle-shaped and have high motility and migratory abilities, while epithelial cells are usually round and form layers of cells that maintain cell–cell adhesion. Mesenchymal cells can convert into epithelial cells and *vice versa* by processes known as MET and epithelial-to-mesenchymal transition (EMT), respectively; both processes being fundamental to development.^{19,20} MET and EMT were shown to have roles in metastasis as well; while EMT contributes to invasion and dissemination, MET is important for colonization at distant sites.²¹ As mentioned, MET is evident during the initial phase of reprogramming. Li *et al.*¹⁷ reported that Sox2 and Oct4 repress the transcription of the master EMT inducer *Snai1*, while Klf4 augments the epithelial program by directly inducing the expression of epithelial genes, and primarily, E-Cadherin (*Cdh1*).

Klf4 is a zinc-finger transcription factor that regulates diverse processes such as proliferation, differentiation and apoptosis; and can either activate or repress gene transcription.²² For example, while overexpression of Klf4 can transactivate p21, it can also transcriptionally repress p53.²³ In addition, Klf4 was reported to act as a tumor suppressor or an oncogene in a context-dependent manner.²² Importantly, as Klf4 is involved in the maintenance of epithelial tissues,²⁴ it may facilitate reprogramming by driving fibroblasts into an epithelial-like state. As described above, during reprogramming, Klf4 induces the transcription of E-Cadherin, a transmembrane protein important for cell–cell adhesion and for determining and maintaining an epithelial phenotype.²⁵ E-Cadherin is dramatically upregulated during the early stages of reprogramming and is required for cell–cell contacts in the forming iPSCs.²⁶ E-Cadherin is also essential in the maintenance of undifferentiated ESCs.²⁷ Accordingly, Chen *et al.*²⁶ demonstrated that E-Cadherin knockdown impairs the formation of iPSCs and its ectopic expression increases reprogramming efficiency.

As described above, p53 regulates a wide variety of the processes that underlie the complex path of reprogramming. While p53-regulated functions such as cell-cycle arrest, senescence and cell death were previously linked to reprogramming, the possibility that p53 affects the very first

and pivotal stage of reprogramming, namely MET, was not explored. Recent studies revealed a role for p53 in controlling EMT, the reverse process of MET. For example, p53-deficient pancreatic cells lose their epithelial characteristics and undergo EMT under stress conditions.²⁸ Additionally, the reduction in p53 expression is necessary for neural crest delamination, an EMT-mediated process.²⁹ These findings position p53 at the junction between epithelial and mesenchymal differentiation states. Therefore, we sought to specifically uncover the putative involvement of p53 in MET during reprogramming. Indeed, we found that in mouse embryonic fibroblasts (MEFs), deletion of p53 profoundly augments E-Cadherin induction during reprogramming with Oct4, Sox2 and Klf4, as well as following ectopic expression of Klf4 alone. The inhibitory effect of p53 was not restricted to E-Cadherin expression, but was rather observed for a large set of Klf4-induced epithelial genes. Moreover, we found that even before ectopic expression of reprogramming factors, mesenchymal cells with attenuated p53 activity display an increase in the expression of epithelial genes. Interestingly, we revealed that the MET-suppressive activity of p53 is mediated by p21. Taken together, these results demonstrate an additional mechanism by which the p53–p21 axis can restrain somatic cell reprogramming and restrict cellular plasticity.

Results

p53 abrogation facilitates MET during the early stages of reprogramming. Recent studies revealed that during the initial phase of reprogramming, MEFs undergo MET.^{16,17} To elucidate whether p53 affects this process, we infected p53^{+/+} and p53^{-/-} MEFs with retroviruses encoding Oct4, Sox2 and Klf4. In agreement with previous reports,^{9–14} loss of p53 increased the reprogramming efficiency, as colonies with ESC-like morphology appeared 10 days post-infection in p53^{-/-} cells compared with day 21 in p53^{+/+} cells (data not shown). On day 19 post-infection, p53^{-/-} cells yielded higher number of Alkaline Phosphatase-positive colonies compared with their p53^{+/+} counterparts (Figure 1a).

Expression of E-Cadherin is a hallmark of epithelial cells.²⁵ Accordingly, E-Cadherin is upregulated during MET, and its induction is crucial for reprogramming.^{17,26} We therefore evaluated MET by QRT-PCR measurements of E-Cadherin mRNA levels. We revealed that compared with p53^{+/+} cells, p53^{-/-} cells exhibit higher induction of E-Cadherin at each of the analyzed time points (Figure 1b). Since the most pronounced induction of E-Cadherin was observed on day 9, we measured the expression of additional epithelial markers, including *Krt8*, *Ocln*, *Dsp* and *Epcam*, at this time point. All markers showed similar expression patterns as E-Cadherin, reaching markedly higher levels in p53^{-/-} cells compared with p53^{+/+} cells (Figure 1c). While the induction of epithelial genes was strongly attenuated by p53, the expression of mesenchymal markers such as N-Cadherin and Fibronectin was comparable between p53^{+/+} and p53^{-/-} cells at day 9 post-infection (data not shown). These results indicate that during reprogramming, p53^{-/-} MEFs activate the transcription of epithelial genes earlier and to a greater extent compared with p53^{+/+} MEFs, which can explain,

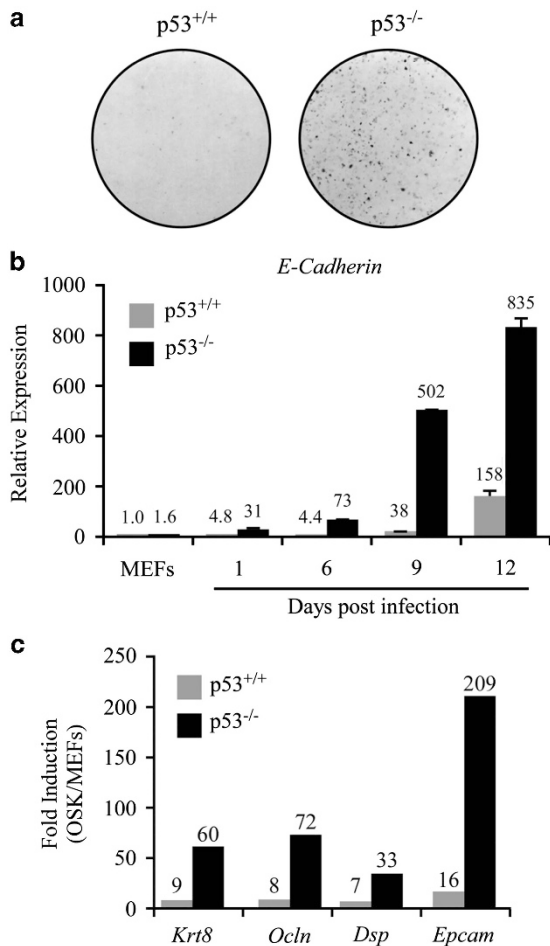


Figure 1 Loss of p53 facilitates MET during early stages of reprogramming. (a) p53^{+/+} and p53^{-/-} MEFs that were infected with retroviruses encoding the reprogramming factors Oct4, Sox2 and Klf4 (OSK) were assayed for alkaline phosphatase activity 19 days post-infection. (b) E-Cadherin mRNA levels, measured by QRT-PCR, in non-infected and OSK-infected p53^{+/+} and p53^{-/-} MEFs at the indicated days post-infection. (c) mRNA fold induction of epithelial markers Keratin 8 (*Krt8*), Occludin (*Ocln*), Desmoplakin (*Dsp*) and Epithelial cell adhesion molecule (*Epcam*), measured by QRT-PCR, in OSK-infected p53^{+/+} and p53^{-/-} MEFs at day 9 post-infection relative to non-infected MEFs

at least in part, the contribution of p53 loss to enhanced reprogramming efficiency.

Loss of p53 facilitates Klf4-induced MET. As part of the MET that underlies reprogramming, the suppression of the mesenchymal transcriptional program is orchestrated by Sox2 and Oct4, whereas the activation of the epithelial program is primarily executed by Klf4.¹⁷ Since we observed a stronger p53 dependency in the activation of the epithelial program, we focused our following experiments on the role of p53 in regulating Klf4-induced MET. To this end, we infected p53^{+/+} and p53^{-/-} MEFs with either control retroviruses or with retroviruses encoding Klf4. For all further analyses, pools of infected cells were used.

Few reciprocal interactions between Klf4 and p53 were previously reported, including the ability of Klf4 to repress p53 transcription,³⁰ and the ability of p53 to transactivate *Klf4*.³¹

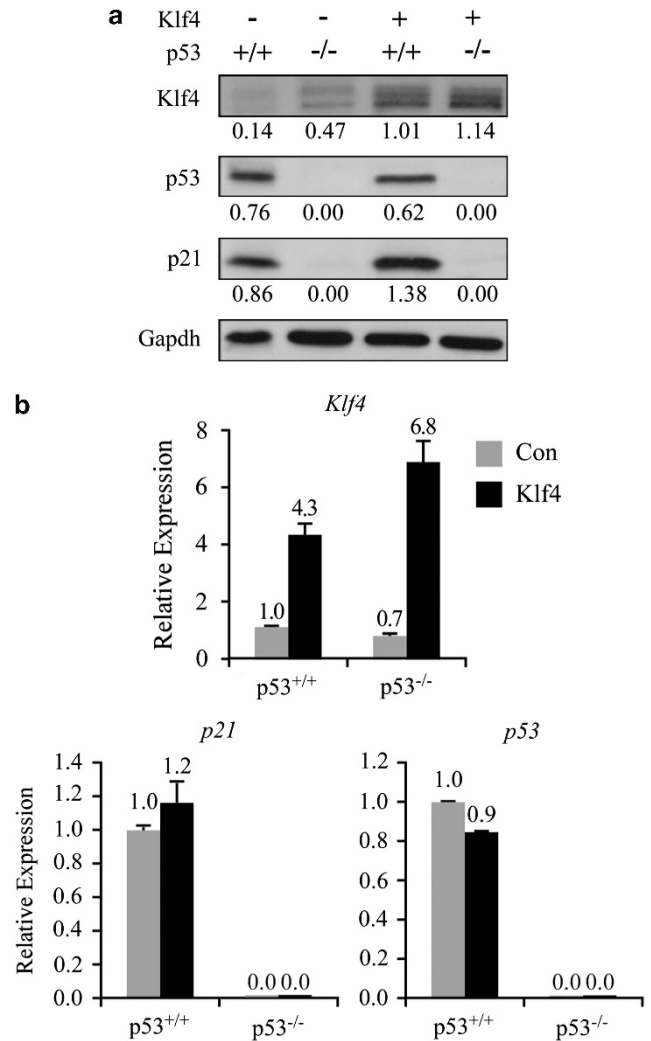


Figure 2 Klf4 and p53 do not affect each other's expression. p53^{+/+} and p53^{-/-} MEFs were stably infected with either control (Con) or Klf4-encoding retroviruses (Klf4). (a) Protein levels of p53, p21 and Klf4 were measured by western blot analysis. GAPDH serves as loading control. Numbers below bands represent normalized intensity, which was calculated by dividing the intensity of each band, quantified using ImageJ, by the respective intensity of GAPDH. (b) QRT-PCR measurements were conducted for p53, p21 and Klf4 mRNA levels

As shown in Figure 2, Klf4 overexpression did not dramatically alter the levels of p53 or its target, p21. Klf4 protein level, but not mRNA, was higher in p53^{-/-} MEFs compared with p53^{+/+} MEFs. However, Klf4 overexpression led to comparable Klf4 mRNA and protein levels in p53^{+/+} and p53^{-/-} MEFs, indicating that any observed effect of p53 on Klf4-induced MET is exerted downstream of Klf4 expression and stability.

Next, the expression of E-Cadherin was evaluated following stable Klf4 overexpression, revealing a profound dependency on p53 presence, that is, E-Cadherin was moderately induced (5.6-fold) by ectopic Klf4 in p53^{+/+} cells compared with a robust elevation (110-fold) in p53^{-/-} cells (Figure 3a). Additionally, loss of p53 and overexpression of Klf4 synergized in the induction of E-Cadherin protein and its

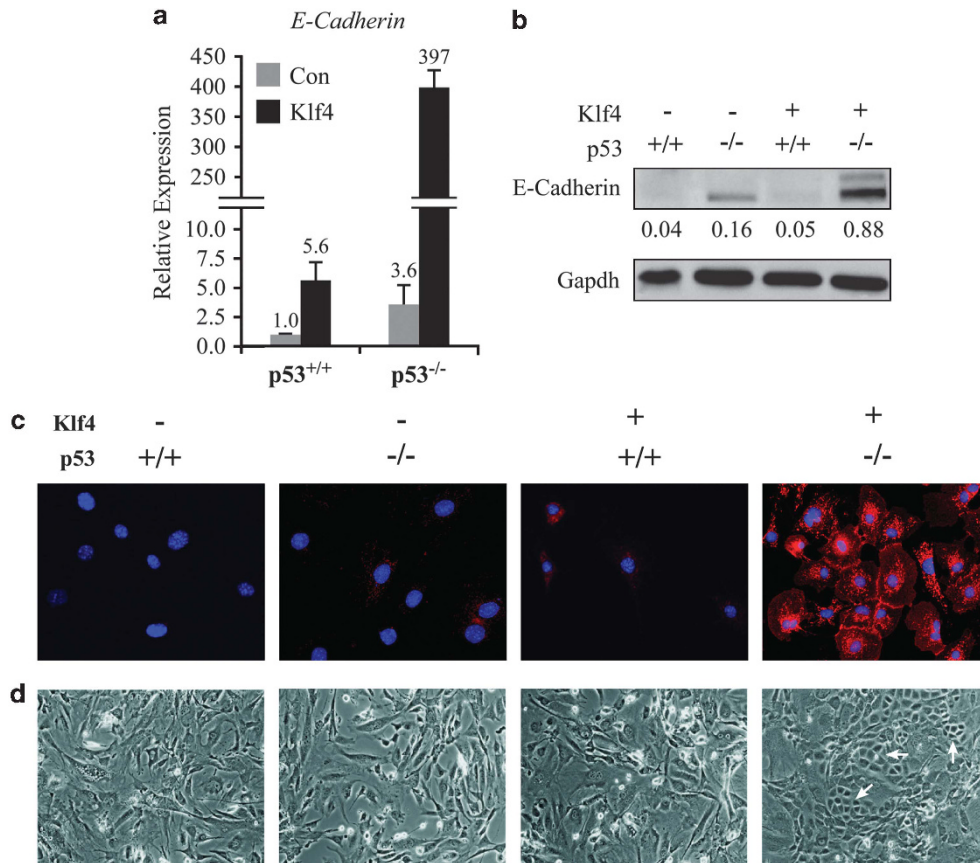


Figure 3 Loss of p53 and Klf4 overexpression cooperatively induce MET. p53^{+/+} and p53^{-/-} MEFs were stably infected with either control (Con) or Klf4-encoding retroviruses (Klf4). (a) QRT-PCR measurements of E-Cadherin mRNA level. (b) The western blot presented in Figure 2a was probed with an antibody against E-Cadherin. GAPDH protein levels are displayed again for convenience. Numbers below bands represent normalized intensity, which was calculated by dividing the intensity of each band, quantified using ImageJ, by the respective intensity of GAPDH. (c) Immunofluorescence staining of E-Cadherin. DNA is counterstained with DAPI. (d) Phase-contrast images of cell cultures. Arrows indicate areas of typical epithelial morphology, defined by tightly arranged foci of rounded cells

organization along cell–cell junctions (Figures 3b and c). Finally, we monitored alterations in cellular morphology following Klf4 overexpression and detected areas with epithelial-like morphology in p53^{-/-} cells expressing Klf4, but not in Klf4-expressing p53^{+/+} cells (Figure 3d). Notably, these results were obtained in four independent experiments, using various batches of MEFs isolated from two independently bred mouse colonies. Ectopic Klf4 expression levels in p53^{+/+} and p53^{-/-} cells were comparable in all experiments, excluding the possibility that the enhanced MET of Klf4-infected p53^{-/-} cells stems from increased infection yield or batch effects.

p53 inhibits E-Cadherin expression in mouse mesenchymal cells. In the above-mentioned experiments, we noticed that even before Klf4 overexpression, the levels of E-Cadherin mRNA and protein are consistently higher in p53^{-/-} MEFs compared with p53^{+/+} MEFs (Figures 3a–c). These results suggest that p53 represses E-Cadherin expression at basal levels. To further validate this phenomenon, we stably knocked-down p53 in p53^{+/+} MEFs. Despite the moderate efficiency of p53 knockdown, E-Cadherin expression was increased 3.7-fold (Figure 4a). Next, we tested

whether p53-dependent repression of E-Cadherin is a general phenomenon to mesenchymal cells by knocking-down p53 in three mesenchymal cell lines that express wild-type p53: the osteogenic cell line MBA-15, the fibroblast line NIH3T3 and the multipotent mesenchymal line C3H10T1/2. Consistently, E-Cadherin level was upregulated following p53 knockdown in these lines (Figure 4a). We then treated p53^{+/+} and p53^{-/-} MEFs with Nutlin-3a, a compound which impairs Mdm2–p53 interaction, thereby stabilizing and activating p53. Nutlin-3a treatment led to a p53-dependent downregulation of E-Cadherin expression (Figure 4b); supporting the notion that p53 transcriptionally represses E-Cadherin.

Of note, we occasionally observed that the level of the endogenous Klf4 protein, but not mRNA, was higher in p53^{-/-} MEFs compared with p53^{+/+} MEFs (Figure 2). This may imply that the increased expression of E-Cadherin in p53^{-/-} cells stems from elevated Klf4 level. However, efficient knockdown of Klf4 in these cells did not lead to E-Cadherin downregulation (Supplementary Figure 1), indicating that a different mechanism is responsible for the augmented expression of E-Cadherin in p53-compromised cells.

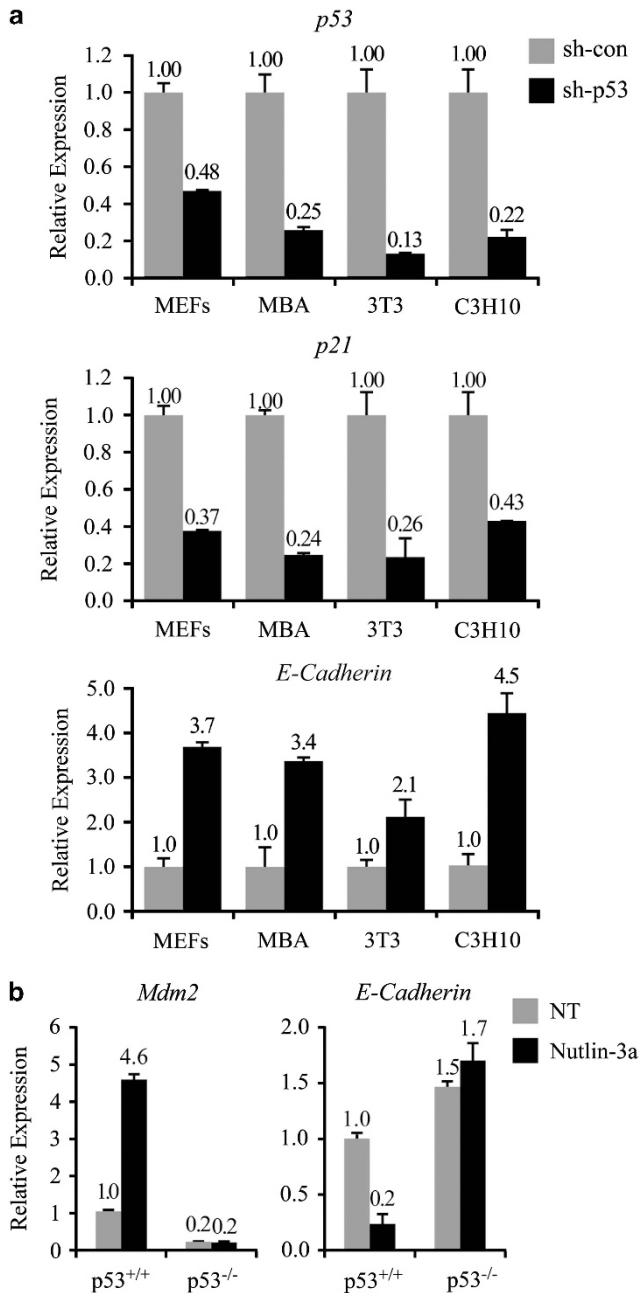


Figure 4 Expression of E-Cadherin negatively correlates with p53 and p21 levels in mouse mesenchymal cells. (a) QRT-PCR measurements for p53, p21 and E-Cadherin mRNA levels in MEFs, MBA-15 (MBA), NIH3T3 (3T3) and C3H10T1/2 (C3H10) cells expressing either a control shRNA (sh-con) or a shRNA targeting p53 (sh-p53). (b) p53^{+/+} and p53^{-/-} MEFs were treated with 25 μ M Nutlin-3a for 16 h. Non-treated (NT) cells were used as controls. mRNA levels of Mdm2 and E-Cadherin were measured by QRT-PCR. Expression levels of Mdm2, a transcriptional target of p53, were analyzed as a measure for p53 activation

p53 deletion and Klf4 overexpression cooperate in the activation of a transcriptional signature enriched with epithelial genes. The observation that p53 restricts Klf4-induced MET prompted us to further explore this role of p53 by investigating genome-wide expression profiles. For this purpose, RNA samples from control or Klf4-infected p53^{+/+} and p53^{-/-} cells were analyzed using cDNA microarrays.

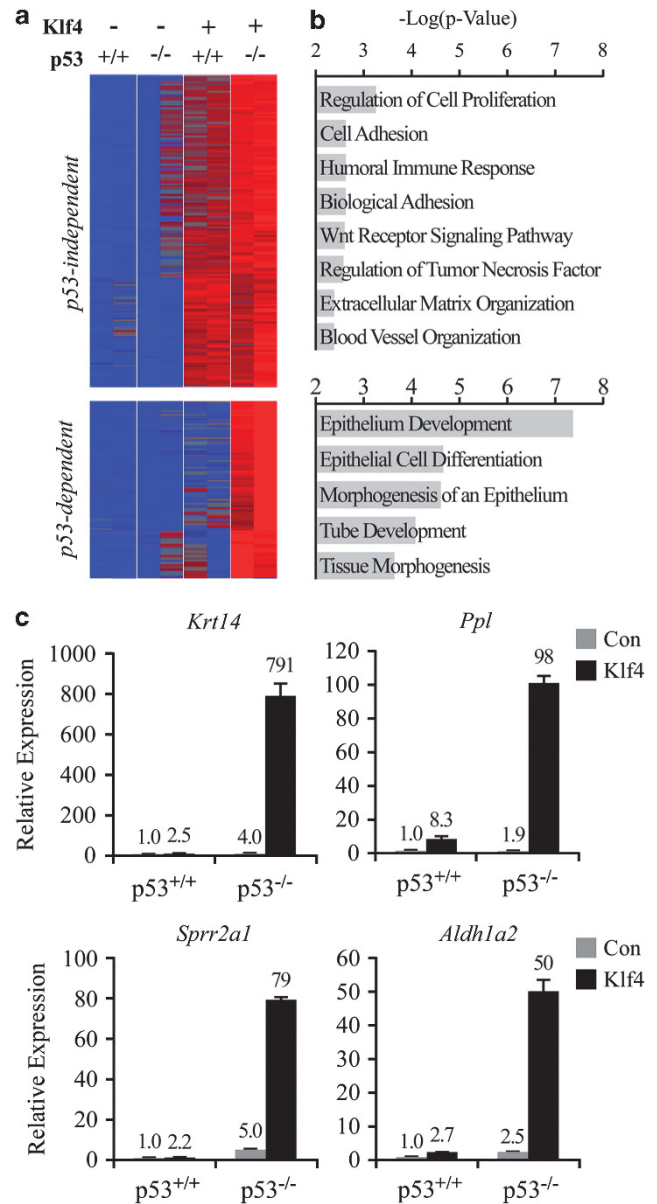


Figure 5 Loss of p53 facilitates Klf4-induced expression of epithelial genes. (a) Heatmap representation (red: high; blue: low) of standardized Affymetrix microarray data depicting log₂ intensity of Klf4-induced genes in p53^{+/+} and p53^{-/-} MEFs introduced with ectopic Klf4. 'p53-independent' (top) and 'p53-dependent' (bottom) clusters are presented. (b) Gene enrichment analysis for the two clusters. Bars correspond to -Log₁₀(P-value) for each enriched category. (c) QRT-PCR validation of expression patterns of Keratin 14 (Krt14), Perioplakin (Ppl), Small proline-rich protein 2A1 (Spr2a1) and Aldehyde Dehydrogenase 1A2 (Aldh1a2)

Analysis of variance identified two distinct sets of Klf4-induced genes (Supplementary Table 1). The first set, designated as the 'p53-independent cluster', comprised 203 genes that were upregulated by Klf4 in both p53^{+/+} and p53^{-/-} cells. The second group termed the 'p53-dependent cluster', included 138 genes that were induced by Klf4 almost exclusively in p53^{-/-} cells. As depicted in Figure 5b, gene enrichment analysis revealed that while the 'p53-independent cluster' was not enriched in any functional category

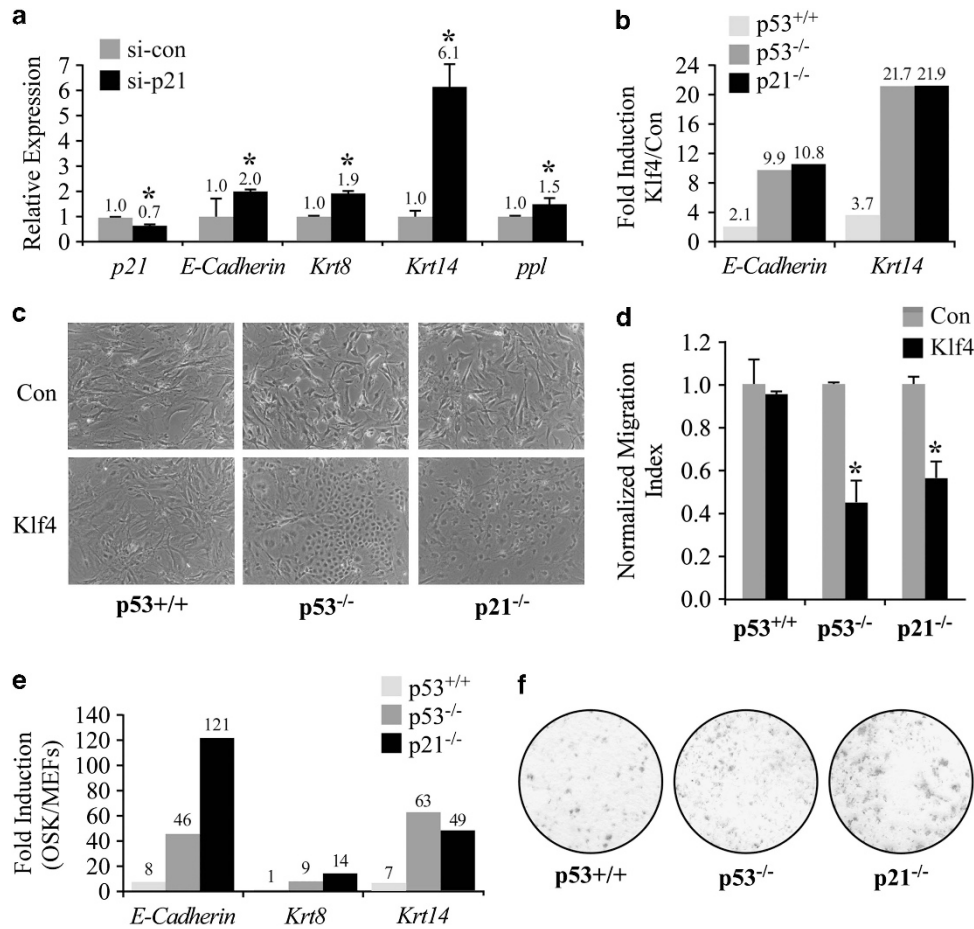


Figure 6 p21 mediates p53-dependent inhibition of MET. (a) p53^{+/+} MEFs were transiently transfected with small interfering RNA oligonucleotides targeting p21 (si-p21) or a non-targeting control (si-con). QRT-PCR was performed 2 days post-transfection. Asterisks denote statistical significant difference (P -value < 0.05) between si-con and si-p21 cells. (b–d) p53^{+/+}, p53^{-/-} and p21^{-/-} MEFs were stably infected with either control (Con) or Klf4-encoding retroviruses (Klf4) and grown for 7 days. QRT-PCR analysis was performed for E-Cadherin and Krt14. Values represent fold induction compared with control-infected cells (b). Phase-contrast images of cell cultures (c). Migration assay was performed for p53^{+/+}, p53^{-/-} and p21^{-/-} cells (d). Migration Index represents fold change in migratory capacity of Klf4-infected cells compared with Con cells. Asterisks denote statistical significant difference (P -value < 0.05) between Con and Klf4 cells. (e) mRNA fold induction of epithelial markers E-Cadherin, Krt8 and Krt14, measured by QRT-PCR, in OSK-infected p53^{+/+}, p53^{-/-} and p21^{-/-} MEFs at day 7 post-infection relative to non-infected MEFs. (f) OSK-infected MEFs were assayed for alkaline phosphatase activity 15 days post-infection

beyond a permissive threshold of P -value < 10^{-4} , the ‘p53-dependent cluster’ was enriched in several categories related to epithelium development and function, the most notable of which was ‘epithelium development’ (P -value = 4.2×10^{-8}). QRT-PCR analysis of candidate epithelial genes from this category, including Krt14, Ppl, Sprr2a1 and Ecam, confirmed the cooperation between p53 absence and Klf4 in the transactivation of epithelial genes. Moreover, similar to E-Cadherin, these epithelial genes were upregulated in p53^{-/-} MEFs compared with p53^{+/+} MEFs even in the absence of ectopic Klf4. Last, according to published ChIP-Seq,³² Krt14, Aldh1a2 and Ppl loci are bound by Klf4, indicating that they are direct transcriptional targets of Klf4.

Next, we analyzed the expression patterns of the ‘p53-dependent cluster’ genes in an expression data set published by Li et al.,¹⁷ who tested how reprogramming is affected by TGF β , a master inducer of EMT and, accordingly, an inhibitor of MET. We found that among the ‘p53-dependent cluster’ genes, a statistically significant portion (22%, P -value = 5.38

$\times 10^{-7}$) is downregulated during reprogramming in TGF β -treated cells. This result confirms that a significantly large portion of genes that are cooperatively induced by ectopic Klf4 and p53 loss participate in the MET program, further supporting the notion that p53-counteracts Klf4-induced MET.

p53-dependent inhibition of MET is mediated by p21.

The majority of the inhibitory functions of p53, including cell-cycle arrest and senescence, is primarily mediated by the induction of p21. Moreover, p53-dependent transcriptional repression is largely exerted by p21.^{2,33} We therefore tested whether the inhibitory function of p53 on MET is p21-dependent. Mild transient knockdown of p21 in p53^{+/+} MEFs resulted in induction of epithelial markers such as E-Cadherin, Krt8, Krt14 and ppl (Figure 6a). Following Klf4 overexpression, the induction of representative epithelial genes such as E-Cadherin and Krt14 was markedly similar between p21^{-/-} and p53^{-/-} MEFs, and was significantly higher compared with p53^{+/+} MEFs (Figure 6b). Similar to

p53^{-/-} MEFs, p21^{-/-} MEFs were also more susceptible than p53^{+/+} MEFs to Klf4-induced MET, as demonstrated by acquisition of an epithelial morphology (Figure 6c). Furthermore, since motility is a phenotypic hallmark of mesenchymal cells, MET should result in attenuated motility. We therefore assessed the effect exerted by Klf4 on the motility of p53^{+/+}, p53^{-/-} and p21^{-/-} cells using a transwell migration assay (Figure 6d). Supporting our hypothesis, Klf4 overexpression had negligible effect on p53^{+/+} cells, while the migratory capacities of p53^{-/-} and p21^{-/-} cells were significantly attenuated by Klf4 (P -value < 0.05). The Klf4-dependent reduction in migratory ability in p53^{-/-} cells was also observed in a wound healing assay (Supplementary Figure 2a). Finally, loss of p21 also facilitated MET upon induction of reprogramming by Oct4, Sox2 and Klf4 (OSK), as evident by the robust induction of epithelial genes 7 days post-infection (Figure 6e; Supplementary Figure 2b). This augmented MET likely facilitates the observed enhancement of reprogramming efficiency of p21^{-/-} MEFs, as assessed by Alkaline Phosphatase activity (Figure 6f), and in agreement with other reports.^{11–14} The aforementioned results indicate that the p53-dependent suppression of MET is primarily mediated by p21.

Discussion

Recently, p53 was shown to function as a barrier for somatic cell reprogramming,^{9–14} a process of complete de-differentiation. As recent papers report that MET is an initial and a necessary step in the reprogramming of MEFs,^{16,17} we sought to examine whether this form of de-differentiation is regulated by p53. We found, as expected, that p53^{-/-} MEFs are more prone to reprogramming, but more interestingly, that they also display an earlier onset and stronger induction of epithelial markers (Figure 1). Our data further demonstrate that Klf4 and p53 deficiency act cooperatively in the activation of an epithelial transcriptional program, acquisition of epithelial morphology and reduction in motility. Importantly, the repressive effect of p53 on the transcription of epithelial genes is observed as early as 1 day following infection with reprogramming factors (Figure 1a), as well as in cells that stably express ectopic Klf4 and are grown in the presence of a selection drug, indicating that the MET-inhibitory effect of p53 is not mediated by its ability to modulate proliferation, senescence, immortalization or apoptosis. Therefore, our results suggest a novel role for p53, by which it counteracts reprogramming via inhibition of Klf4-induced MET.

We also report that in diverse types of mesenchymal cells, loss of p53, in the absence of any additional manipulations, leads to an increase in the expression of epithelial genes (Figures 4 and 5). Interestingly, a recent article reports an opposite phenomenon using epithelial cells from ovarian tumors, where inhibition of p53 results in E-Cadherin down-regulation.³⁴ This apparent contradictory effect may be explained if one considers p53 as a homeostasis gene that restricts cell plasticity. As such, p53 may inhibit E-Cadherin expression in mesenchymal cells while maintaining high E-Cadherin levels in epithelial cells. This notion also agrees with the observation that in epithelial cells, p53 inhibits EMT,^{28,29} while our data indicate that in mesenchymal cells,

it attenuates MET. The opposing effects of p53 on E-Cadherin expression suggest an indirect mechanism by which p53 regulates E-Cadherin transcription. Indeed, deletion of p21 had a strikingly similar MET-facilitating effect as deletion of p53 (Figure 6), suggesting that p53-dependent inhibition of MET is mediated primarily by p21. We hypothesize that the p53–p21 axis reduces cellular plasticity via multiple downstream mechanisms, including inhibition of cell-cycle progression and chromatin reorganization. Further studies are required to elucidate the circuitry linking p53 and the EMT/MET regulatory network.

iPSC generation can be enhanced by overexpressing E-Cadherin, whereas knockdown of E-Cadherin inhibits reprogramming.²⁶ In addition, epithelial cells can generally be reprogrammed more efficiently than mesenchymal cells.^{17,18} Thus, the observed activation of an epithelial-like program in mesenchymal cells with compromised p53 may further explain how such cells are more prone to reprogramming. Interestingly, p53-deficient MEFs can be reprogrammed with only Oct4 and Sox2, albeit at very low efficiency.^{12,15} Therefore, although p53 reduction does not completely substitute for Klf4 in reprogramming, the increase in E-Cadherin expression in p53-deficient MEFs possibly exceeds a threshold sufficient for iPSC generation in the absence of Klf4.

Our data suggest that p53 acts to maintain the identity of mesenchymal cells. This activity may be important both in normal development, as demonstrated in *Xenopus laevis*, where p53-deficient embryos exhibit inhibition of mesodermal differentiation and severe gastrulation defects,³⁵ and in the context of tumorigenesis. Both reprogramming and oncogenic transformation require specific combinations of genes to generate less differentiated cells with increased self-renewal capacity. This similarity may provide insights into the mechanisms of tumorigenesis. Given the ability of p53 to restrict MET during reprogramming; and the frequent mutation of p53 during tumorigenesis, it is reasonable to assume that p53 loss during cancer progression facilitates de-differentiation in a similar fashion as in reprogramming. Indeed, a correlation between ESC expression signatures and p53 mutations in breast cancer was reported,³⁶ supporting the notion that p53 loss enables developmental plasticity and facilitates the acquisition of a stem-like state.

The role of Klf4 in tumor formation and progression is controversial, as Klf4 was reported to act both as a tumor suppressor and an oncogene, depending on the cellular context.²² This duality may be modulated by additional cellular factors, one of which may be the status of p53. Similarly, p53 status greatly affects cellular responses to the introduction of key transcription factors or signaling components, such as oncogenic Ras,³⁷ which induces senescence in p53-proficient cells, but can transform p53-deficient cells. Importantly, a functional link between p53 and Klf4 was demonstrated in transgenic mice, in which expression of Klf4 in the basal layer of the epidermis induces hyperplasia/dysplasia on a p53^{+/+} background, whereas on a p53^{+/-} background, these mice develop sarcomas.³⁸ Moreover, Klf4-overexpressing p53^{-/-} MEFs generate malignant tumors in nude mice, while control p53^{-/-} MEFs do not grow *in vivo*.¹⁵ Our data may provide mechanistic insights into these phenomena as we demonstrate that p53 exerts a genome-wide inhibition of the

Klf4-induced transcriptional program, which may restrict, and even revert, Klf4 oncogenic potential.

The capacity of p53 to regulate fundamental cellular processes such as cell-cycle arrest, apoptosis and senescence is well described. However, if, and how, p53 loss bestows cells with stem cell-like properties, as well as the ability to metastasize is poorly understood. It is becoming evident that metastatic cells display properties of EMT, and subsequently, the disseminated cells must undergo MET at the site of metastases. This suggests that cellular plasticity is a key feature of metastasis. In this study, we provide a link between p53 loss and the MET process, improving our understanding of the early steps of reprogramming, as well as tumor formation and metastasis.

Materials and Methods

Cell culture. Primary MEFs were prepared from 13.5 dpc embryos derived from p53^{+/+} and p53^{-/-} sibling C57BL/6 mice. Embryos were dissected to remove the digestive tract. The dissected tissues were treated with 0.25% trypsin and EDTA. Trypsinization was held in three cycles, 20 m each. After each cycle the semi-liquid portion was transferred to a 50-ml tube and neutralized by adding the same volume of growth medium containing fetal calf serum (FCS). The rest of the material was left for another cycle, using fresh trypsin. The tubes were centrifuged at 2000 r.p.m. for 5 m, the supernatant was aspirated and pellets were resuspended in growth medium and seeded on 10 cm tissue culture plates. p21^{-/-} MEFs were kindly provided by Dr. G. Lozano (University of Texas M.D. Anderson Cancer Center). MEFs were maintained in DMEM, supplemented with 10% FCS, 1 mM sodium pyruvate, 2 mM L-Glutamine and 100 mg/ml penicillin/streptomycin. MBA-15 cells, kindly provided by Dr. Zipori (Weizmann Institute, Israel), as well as NIH3T3 and C3H10T1/2 (ATCC, Rockville, MD, USA) were cultured in DMEM supplemented with 10% FCS and 100 mg/ml penicillin/streptomycin. iPSCs were cultured in ES medium (DMEM supplemented with 15% FCS, 1 mM sodium pyruvate, 2 mM L-Glutamine, 0.1 mM non-essential amino acids, 0.1 mM β -mercaptoethanol, 1000 units/ml Leukemia Inhibitory Factor (ESG1107, Millipore, Billerica, MA, USA) and penicillin/streptomycin). The ecotropic Phoenix retrovirus-producing cells were obtained from the ATCC. All cell lines were grown at 37 °C in a humidified atmosphere of 5% CO₂.

Retroviral constructs, infections and transfections. pMXs- mouse Sox2, Oct4 and Klf4 expression constructs⁸ were purchased from Addgene (Cambridge, MA, USA). For Klf4 overexpression, the mouse Klf4 coding sequence from pMXs-Klf4 was subcloned into a pBabe-hygro vector using *EcoRI*. For p53 knockdown, mouse-specific p53 short hairpin RNA (sh-p53) vector and human-specific RB1 shRNA control (sh-con) vector were used (kindly provided by Dr. S.W. Lowe, Cold Spring Harbor Laboratory, NY, USA). Ecotropic Phoenix-packaging cells were transfected with the appropriate retroviral construct by a standard calcium phosphate procedure. Culture supernatants were collected 48 h post-transfection and filtered. Recipient cells were infected with the filtered viral supernatants in the presence of 4 μ g/ml polybrene (Sigma, Rehovot, Israel) four times in 12 h intervals. Cells infected with pBabe-hygro-Klf4 or pBabe-hygro were maintained in 100 μ g/ml hygromycin B containing medium to sustain Klf4 overexpression. Cells infected with sh-p53 or sh-con vectors were selected with 1 μ g/ml Puromycin for 1 week. For transient knockdown of p21 and Klf4, subconfluent cells were transfected with siGENOME smart pools (Dharmacon, Lafayette, CO, USA) using DharmaFECT3 according to manufacturer protocol.

iPSCs generation. To generate iPSCs, MEFs were infected with pMXs vectors encoding mouse Oct4, Sox2 and Klf4 and following 24 h, 3.5×10^5 cells were seeded on irradiated (60 gray) feeder MEFs in ES media. Emerging colonies were selected based on ES-like morphology and isolated for further characterization.

Immunofluorescent staining. Cells were seeded on glass cover slips and incubated for 48 h. Cells were then fixed with 4% paraformaldehyde (Santa Cruz Biotechnology, Santa Cruz, CA, USA) in PBS for 15 m, washed three times with PBS and permeabilized with 0.2% Triton X-100 in PBS for 5 m. Cells were blocked with PBS containing 0.1% Triton and 3% normal goat serum for 1 h at room

temperature. For immunostaining, cells were incubated for 2 h in room temperature with mouse anti-E-Cadherin (610181, 1:200, BD Biosciences, San Jose, CA, USA) in blocking solution. After three washes with PBS containing 0.1% Triton X-100, cells were incubated for 1 h at room temperature with Cy3-conjugated goat anti-mouse secondary antibody (Jackson ImmunoResearch, Suffolk, UK) and counterstained with 10 μ g/ml 4',6-diamidino-2-phenylindole (DAPI) to visualize nuclei. The cover slips were mounted with elvanol, and the cells were viewed under a fluorescence microscope.

Alkaline phosphatase assay. Cells were washed with PBS, fixed with 4% paraformaldehyde (Santa Cruz Biotechnology), followed by three washes with PBS, and then incubated with alkaline phosphatase reaction buffer (100 mM Tris-HCl pH 8.0, 100 mM NaCl, 20 mM MgCl₂, 0.5 mg/ml Fast Blue (Sigma) and 0.01% Naphtol (Sigma)) for 30 m, followed by washing with PBS.

RNA isolation and quantitative real-time-PCR (QRT-PCR). Total RNA was isolated using NucleoSpin RNA II kit (Macherey-Nagel, Düren, Germany) according to the manufacturer's protocol. A 2- μ g aliquot of the total RNA was reverse transcribed into cDNA using Bio-RT (9597, Bio-Lab, Jerusalem, Israel), dNTPs and random hexamer primers. QRT-PCR was performed on ABI7300 instrument (Applied Biosystems, Carlsbad, CA, USA) using SYBR Green PCR Master Mix (Applied Biosystems) and the specific primers listed in Supplementary Table 2. Data analysis was performed according to the $\Delta\Delta$ Ct method using HPRT as the endogenous control. The results are presented as a mean \pm S.D. of two or three duplicate runs from a representative experiment.

Western blot analysis. Cells were lysed in TLB buffer (50 mM Tris-HCl, 100 mM NaCl, 1% Triton X-100, 0.5% sodium deoxycholate, 0.1% SDS) supplemented with protease inhibitor cocktail (Sigma) for 15 m on ice, followed by centrifugation. BCA reagent (Pierce, Rockford, IL, USA) was used to determine protein concentration. Then, 70 μ g protein of each sample were separated by SDS-PAGE, and transferred to nitrocellulose membranes. Either of the following primary antibodies was used: mouse monoclonal anti-GAPDH (1 : 1000, MAB374, Chemicon International, Billerica, MA, USA), mouse monoclonal anti-p53 (1 : 500, 1c12, Cell Signaling, Danvers, MA, USA), mouse monoclonal anti-p21 (1 : 1000, 556430, BD Biosciences), mouse monoclonal anti E-Cadherin (1 : 1000, 610181, BD Biosciences), rabbit polyclonal anti-Klf4 (1 : 500, H-180, Santa Cruz Biotechnology). The protein-antibody complexes were detected using horseradish peroxidase-conjugated secondary antibodies and the Amersham ECL Western blotting detection reagents (GE Healthcare, Buckinghamshire, UK). Quantification of protein levels was performed using ImageJ (NIH, Bethesda, MD, USA).

Wound healing assay. Cells were seeded in 24-well plates and incubated at 37 °C overnight to generate confluent culture. Cells were then serum-starved for 8 h. Cell layers were scraped with a plastic tip and washed three times with PBS. The remaining cell culture was incubated 20 h to allow migration. Phase-contrast images of identical locations in each wound were taken at 0 and 20 h after wounding. Gap width was quantified with the WimScratch software (Wimasis, Munich, Germany). The percentage of wound closure was calculated by dividing the gap final width by its initial width and subtracting the result from 100%.

Transwell migration assay. Cells were seeded with serum-free media in the top chamber of a CIM-plate 16 (Roche Applied Science, Indianapolis, IN, USA). Media containing 10% FCS were applied to the bottom chamber. Cells were incubated at 37 °C for 4 h, and electrical impedance, which is proportional to the amount of migratory cells, was assessed using xCELLigence Real-Time Cell Analyzer DP instrument (Roche Applied Science) according to the manufacturer's instructions.

Microarray and data analysis. cDNA from two biological replicates of p53^{+/+} and p53^{-/-} MEFs infected with either a control vector or Klf4-encoding vector were labeled using Ambion WT expression kit (Affymetrix, Santa Clara, CA, USA) and hybridized to Affymetrix Mouse Gene 1.0 ST microarray using Affymetrix hybridization kit according to the manufacturer's instructions. Transcriptome analysis was performed using Partek Genome Suite (GS) software V6.5. Preprocessing was performed using the GC-Robust Microarray Averaging algorithm (GC-RMA). Genes that were below detection threshold (log₂ intensity < 5.5) across all samples were filtered out. Two-way ANOVA was performed in order to identify genes that were at least 1.8-fold differentially

expressed with a P -value < 0.05 following Klf4 expression in either p53^{+/+} or p53^{-/-} cells. Log2 intensities were standardized and clustered using a Pearson dissimilarity algorithm (CLICK) from the EXPANDER software³⁹ where homogeneity of the expression was set to 0.9. A heatmap of the clusters was created using Partek. Enrichment of gene ontology terms was examined using DAVID functional annotations tool.⁴⁰ For analysis of TGF β effect on global gene expression, microarray data published by Li *et al.*¹⁷ were downloaded from the GEO database (GSE21064). The proportion of genes among the 'p53-dependent cluster' whose expression level was > 1.5 -fold lower in the TGF β sample compared with the control sample was calculated and statistical significance was assessed using a hypergeometric test.

Conflict of Interest

The authors declare no conflict of interest.

- Vousden KH, Prives C. Blinded by the light: the growing complexity of p53. *Cell* 2009; **137**: 413–431.
- Brosh R, Rotter V. Transcriptional control of the proliferation cluster by the tumor suppressor p53. *Mol Biosyst* 2010; **6**: 17–29.
- Molchadsky A, Rivlin N, Brosh R, Rotter V, Sarig R. p53 is balancing development, differentiation and de-differentiation to assure cancer prevention. *Carcinogenesis* 2010; **31**: 1501–1508.
- Donehower LA, Harvey M, Slagle BL, McArthur MJ, Montgomery CA Jr., Butel JS *et al.* Mice deficient for p53 are developmentally normal but susceptible to spontaneous tumours. *Nature* 1992; **356**: 215–221.
- Armstrong JF, Kaufman MH, Harrison DJ, Clarke AR. High-frequency developmental abnormalities in p53-deficient mice. *Curr Biol* 1995; **5**: 931–936.
- Sah VP, Attardi LD, Mulligan GJ, Williams BO, Bronson RT, Jacks T. A subset of p53-deficient embryos exhibit exencephaly. *Nat Genet* 1995; **10**: 175–180.
- Hu W. The role of p53 gene family in reproduction. *Cold Spring Harb Perspect Biol* 2009; **1**: a001073.
- Takahashi K, Yamanaka S. Induction of pluripotent stem cells from mouse embryonic and adult fibroblast cultures by defined factors. *Cell* 2006; **126**: 663–676.
- Utikal J, Polo JM, Stadtfeld M, Maherali N, Kulalert W, Walsh RM *et al.* Immortalization eliminates a roadblock during cellular reprogramming into iPS cells. *Nature* 2009; **460**: 1145–1148.
- Marión RM, Strati K, Li H, Murga M, Blanco R, Ortega S *et al.* A p53-mediated DNA damage response limits reprogramming to ensure iPS cell genomic integrity. *Nature* 2009; **460**: 1149–1153.
- Li H, Collado M, Villasante A, Strati K, Ortega S, Cañamero M *et al.* The Ink4/Arf locus is a barrier for iPS cell reprogramming. *Nature* 2009; **460**: 1136–1139.
- Kawamura T, Suzuki J, Wang YV, Menendez S, Morera LB, Raya A *et al.* Linking the p53 tumour suppressor pathway to somatic cell reprogramming. *Nature* 2009; **460**: 1140–1144.
- Hong H, Takahashi K, Ichisaka T, Aoi T, Kanagawa O, Nakagawa M *et al.* Suppression of induced pluripotent stem cell generation by the p53–p21 pathway. *Nature* 2009; **460**: 1132–1135.
- Hanna J, Saha K, Pando B, van Zon J, Lengner CJ, Creighton MP *et al.* Direct cell reprogramming is a stochastic process amenable to acceleration. *Nature* 2009; **462**: 595–601.
- Sarig R, Rivlin N, Brosh R, Bornstein C, Kamer I, Ezra O *et al.* Mutant p53 facilitates somatic cell reprogramming and augments the malignant potential of reprogrammed cells. *J Exp Med* 2010; **207**: 2127–2140.
- Samavarchi-Tehrani P, Golipour A, David L, Sung HK, Beyer TA, Datti A *et al.* Functional genomics reveals a BMP-driven mesenchymal-to-epithelial transition in the initiation of somatic cell reprogramming. *Cell Stem Cell* 2010; **7**: 64–77.
- Li R, Liang J, Ni S, Zhou T, Qing X, Li H *et al.* A mesenchymal-to-epithelial transition initiates and is required for the nuclear reprogramming of mouse fibroblasts. *Cell Stem Cell* 2010; **7**: 51–63.
- Aasen T, Raya A, Barrero MJ, Garreta E, Consiglio A, Gonzalez F *et al.* Efficient and rapid generation of induced pluripotent stem cells from human keratinocytes. *Nat Biotechnol* 2008; **26**: 1276–1284.
- Thiery JP, Sleeman JP. Complex networks orchestrate epithelial-mesenchymal transitions. *Nat Rev Mol Cell Biol* 2006; **7**: 131–142.
- Chaffer CL, Thompson EW, Williams ED. Mesenchymal to epithelial transition in development and disease. *Cells Tissues Organs* 2007; **185**: 7–19.
- Polyak K, Weinberg RA. Transitions between epithelial and mesenchymal states: acquisition of malignant and stem cell traits. *Nat Rev Cancer* 2009; **9**: 265–273.
- Evans PM, Liu C. Roles of Kruppel-like factor 4 in normal homeostasis, cancer and stem cells. *Acta Biochim Biophys Sin (Shanghai)* 2008; **40**: 554–564.
- Rowland BD, Bernards R, Peeper DS. The KLF4 tumour suppressor is a transcriptional repressor of p53 that acts as a context-dependent oncogene. *Nat Cell Biol* 2005; **7**: 1074–1082.
- Yori JL, Johnson E, Zhou G, Jain MK, Keri RA. Kruppel-like factor 4 inhibits epithelial-to-mesenchymal transition through regulation of E-cadherin gene expression. *J Biol Chem* 2010; **285**: 16854–16863.
- van Roy F, Bex G. The cell-cell adhesion molecule E-cadherin. *Cell Mol Life Sci* 2008; **65**: 3756–3788.
- Chen T, Yuan D, Wei B, Jiang J, Kang J, Ling K *et al.* E-cadherin-mediated cell-cell contact is critical for induced pluripotent stem cell generation. *Stem Cells* 2010; **28**: 1315–1325.
- Soncin F, Mohamet L, Eckardt D, Ritson S, Eastham AM, Bobola N *et al.* Abrogation of E-cadherin-mediated cell-cell contact in mouse embryonic stem cells results in reversible LIF-independent self-renewal. *Stem Cells* 2009; **27**: 2069–2080.
- Pinho AV, Rooman I, Real FX. p53-dependent regulation of growth, epithelial-mesenchymal transition and stemness in normal pancreatic epithelial cells. *Cell Cycle* 2011; **10**: 1312–1321.
- Rinon A, Molchadsky A, Nathan E, Yovel G, Rotter V, Sarig R *et al.* p53 coordinates cranial neural crest cell growth and epithelial-mesenchymal transition/delamination processes. *Development* 2011; **138**: 1827–1838.
- Rowland BD, Peeper DS. KLF4, p21 and context-dependent opposing forces in cancer. *Nat Rev Cancer* 2006; **6**: 11–23.
- Zhang W, Geiman DE, Shields JM, Dang DT, Mahatan CS, Kaestner KH *et al.* The gut-enriched Kruppel-like factor (Kruppel-like factor 4) mediates the transactivating effect of p53 on the p21WAF1/Cip1 promoter. *J Biol Chem* 2000; **275**: 18391–18398.
- Chen X, Xu H, Yuan P, Fang F, Huss M, Vega VB *et al.* Integration of external signaling pathways with the core transcriptional network in embryonic stem cells. *Cell* 2008; **133**: 1106–1117.
- Brosh R, Shalgi R, Liran A, Landan G, Korotayev K, Nguyen GH *et al.* p53-repressed miRNAs are involved with E2F in a feed-forward loop promoting proliferation. *Mol Syst Biol* 2008; **4**: 229.
- Cheng JC, Auersperg N, Leung PCK. Inhibition of p53 represses E-cadherin expression by increasing DNA methyltransferase-1 and promoter methylation in serous borderline ovarian tumor cells. *Oncogene* 2011; **30**: 3930–3942.
- Cordenonsi M, Dupont S, Maretto S, Insinga A, Imbranco C, Piccolo S. Links between tumor suppressors: p53 is required for TGF-beta gene responses by cooperating with Smads. *Cell* 2003; **113**: 301–314.
- Mizuno H, Spike BT, Wahl GM, Levine AJ. Inactivation of p53 in breast cancers correlates with stem cell transcriptional signatures. *Proc Natl Acad Sci USA* 2010; **107**: 22745–22750.
- Solomon H, Brosh R, Buganim Y, Rotter V. Inactivation of the p53 tumor suppressor gene and activation of the Ras oncogene: cooperative events in tumorigenesis. *Discov Med* 2010; **9**: 448–454.
- Foster KW, Liu Z, Nail CD, Li X, Fitzgerald TJ, Bailey SK *et al.* Induction of KLF4 in basal keratinocytes blocks the proliferation-differentiation switch and initiates squamous epithelial dysplasia. *Oncogene* 2005; **24**: 1491–1500.
- Sharan R, Maron-Katz A, Shamir R. CLICK and EXPANDER: a system for clustering and visualizing gene expression data. *Bioinformatics* 2003; **19**: 1787–1799.
- Huang da W, Sherman BT, Lempicki RA. Systematic and integrative analysis of large gene lists using DAVID bioinformatics resources. *Nat Protoc* 2009; **4**: 44–57.

Supplementary Information accompanies the paper on Cell Death and Differentiation website (<http://www.nature.com/cdd>)